Experimental Approach for Measuring Burn Efficiency of a Reduced-Scale Wellhead Fire

May 11-14, 2020

Brian T. Fisher, Steven G. Tuttle, Christopher J. Pfützner, David A. Kessler
Naval Research Laboratory
4555 Overlook Avenue, SW
Washington, DC 20375, USA

ABSTRACT

In the case of wellhead blowout, intentional ignition and burning of the gas/oil discharge is one option to prevent oil accumulation on the ground or water surface until the well can be capped. A critical factor that strongly determines the viability of this strategy is the so-called "burn efficiency," which is the fraction of the oil discharge that burns and does not spill to the surrounding area. This includes not only fully burned liquid oil, however, but also any partially burned droplets or char particles that are dispersed in the surrounding air. We therefore refer to this quantity more accurately as "apparent burn efficiency" (ABE). At the Naval Research Laboratory (NRL), we have set up a scaled-down spray flame system that simulates the internal pipe flow and external two-phase spray of a wellhead and therefore allows us to study the details of wellhead spray and fire behavior. In this paper, we describe a method that we have recently developed to measure liquid oil fallout and determine ABE for gas/oil spray flames. We collect oil fallout in weighing cups at strategic locations to construct fallout mass radial profiles, which are then post-processed to estimate total mass of fallen oil. This is compared to the known total liquid oil discharge to determine ABE. We present ABE results for a series of tests, using a single light crude oil, in which oil and gas flow conditions were fixed and the flame was operated both without and with a pilot flame for comparison. In addition, experimental conditions and results are evaluated in terms of applicability to full-scale wellhead fires.

INTRODUCTION

Over the past few decades, artificial islands have been constructed to support oil and gas exploration and production operations in shallow (~15 – 20 meters) offshore U.S. and Canadian Arctic waters. The remote and relatively inaccessible locations of these sites make traditional oil spill cleanup methods difficult, thus voluntary wellhead ignition has been proposed for many years as a potential control/mitigation strategy for blowouts that occur at these facilities. Unpredictable ignition or burn behavior, and in particular poor burn efficiency, could significantly limit the usefulness of this strategy for both operational and safety reasons.

When a wellhead blowout occurs, it typically leads to an uncontrolled release of high-pressure well gas and crude oil. When ignited, the two-phase gas and oil flow forms a high-pressure spray flame, in which the crude oil has two possible primary fates:

(1) Oil droplets that are sufficiently small rapidly evaporate and subsequently burn, forming product gases and fine particulates that disperse readily.

(2) Some portion of the crude oil will be unable to burn and will fall to the ground (referred to as fallout). This can include fresh/unevaporated oil that falls to the ground as large blobs/droplets very close to the wellhead, partially evaporated and/or burned oil that falls to the ground as smaller droplets over a wider area, and combustion residuals (e.g., soot agglomerates, ash, and large unburned hydrocarbons) that fall to the ground over the widest area.

Conditions in the well (namely pressure, temperature, chemistry, and gas/oil ratio), along with external conditions such as ambient temperature, determine whether there is good or poor atomization of oil droplets, i.e., whether the droplets are large/heavy or small/light. Crude oil burn efficiency, defined as the fraction of crude oil mass flowing out of the wellhead that fully evaporates and burns, is a direct result of the atomization quality – poor atomization and

large/heavy oil droplets presumably lead to poor burn efficiency. True burn efficiency is difficult to directly measure, as it requires capturing all of the unburned oil, no matter how well it disperses and no matter how far it travels before falling to the ground. Therefore, for the purposes of practical measurement, there are two quantities that can be defined – apparent burn efficiency (ABE) and fallout fraction (FF). Fallout fraction can be directly measured as the relative fraction of total oil mass flowing out of the well that falls to the ground in the immediate vicinity. Apparent burn efficiency is simply the unity complement of this quantity, or the fraction of oil that does not fall to the ground. This is not a true burn efficiency because it does not account for any crude oil that is dispersed into the atmosphere or carried a long distance away from the well. Under some circumstances, ABE and true burn efficiency could be nearly identical, while in other cases they may be quite different.

In a recent paper, researchers discuss many of the issues related to the use of wellhead ignition as a blowout response strategy, including burn efficiency and its relationship to well conditions and the two-phase flow within the pipe (Siddhamshetty *et al.* 2019). They describe different two-phase flow regimes, which in order from lowest to highest gas flow rate/velocity include so-called bubble flow, slug/plug flow, churn flow, annular flow, and dispersed/misty flow. In annular flow, the gas occupies the majority of the volume and the liquid is confined to a thin film along the wall. Hasan and Kabir discuss the criteria for transition to annular flow in terms of superficial gas velocity, which Siddhamshetty et al. translate to a gas-oil ratio (GOR) of 500 scf/bbl (Hasan and Kabir 2018, Siddhamshetty *et al.* 2019). Oil wells typically have GOR values that exceed this threshold and thus typically involve annular or fully dispersed internal flows.

Annular flow has several defining characteristics, namely the presence of ripples and waves at the film surface, entrainment of liquid droplets into the gas flow, and re-deposition of entrained

droplets into the liquid film (Al-Sarkhi *et al.* 2012, Aliyu *et al.* 2017, Azzopardi 1997, Berna *et al.* 2014, Berna *et al.* 2015, Henstock and Hanratty 1976, Kataoka *et al.* 1983, Kataoka *et al.* 2000, Liu and Bai 2017, Siddhamshetty *et al.* 2019, Simmons and Hanratty 2001, Steimes and Hendrick 2017, Taitel *et al.* 1980, Tatterson *et al.* 1977, Wang *et al.* 2018, Xue *et al.* 2015, Zhang and Hewitt 2017). Droplet entrainment and re-deposition depend on the relative gas and liquid fractions/velocities in the pipe, and the complex interplay of these effects determines whether any of the liquid film persists to the pipe exit or whether the film is entirely eliminated and entrained as droplets (i.e., misty/dispersed flow) (Al-Sarkhi *et al.* 2012, Aliyu *et al.* 2017, Azzopardi 1997, Berna *et al.* 2014, Berna *et al.* 2015, Kataoka *et al.* 2000, Steimes and Hendrick 2017, Tatterson *et al.* 1977, Zhang and Hewitt 2017). The so-called "entrainment fraction" or "entrained droplet fraction" influences the droplet size distribution in the external spray, since any residual film that atomizes exterior to the pipe will likely produce much larger droplets than those that are entrained before exiting the pipe. Siddhamshetty et al. suggest that annular and dispersed flows could produce small droplets that result in efficient burning, but there are no known papers or studies in which these assumptions have been confirmed experimentally (Siddhamshetty *et al.* 2019). For annular flow in particular, it remains unknown whether the larger droplets produced by external atomization of the liquid film are large enough to significantly impact burn efficiency. This is an important aspect of wellhead ignition/burning that requires further investigation.

Given the critical importance of burn efficiency for intentionally-ignited wellhead fires and the complete lack of relevant data, we have developed a test setup and method at the Naval Research Laboratory (NRL) to measure burn efficiency under controlled conditions. The goal is to obtain experimental data for fuels and conditions relevant to real-world petroleum wellhead fires, albeit at reduced scales. We developed a simple burner to mimic a wellhead at smaller scale and devised

a test method in which unburned oil is collected at discrete, strategic locations for a known period of time during a burn test. The spatial distribution of the collected oil is analyzed to determine a reasonable estimate of the total unburned oil during the collection period, which is then compared with the measured total flow rate of oil supplied to the burner to compute an apparent burn efficiency. The primary objective of this initial study was to demonstrate that the developed measurement technique is valid and robust with respect to changes in conditions outside of our control (e.g., weather). Using a light crude oil and a hydrocarbon gas mixture, tests were conducted at one flow condition many times over the course of several weeks during which weather conditions changed considerably. Results show that ABE stayed consistent for these tests, and that the use of a pilot flame for some of the tests had no significant effect on the results.

EXPERIMENTAL SETUP AND METHODS

For this work, we designed a simple burner that creates flow conditions similar to a petroleum wellhead, but at much smaller scale. As shown in Figure 1, the burner is a long, straight stainless steel tube with inner diameter (ID) of 8.5 mm (0.335 inches) and outer diameter of 9.5 mm (0.375 inches). The gas enters at the bottom, while the liquid enters through a tee slightly above the gas entry point. There are two ports designed for measurement of static pressure, at heights of 19 cm (7.5 inches) and 112 cm (44 inches) above the point of liquid entry.

The mixing tee, which was the main focus of the burner design, is detailed in Figure 1b. Liquid enters through the side-arm and is forced through a group of small (1-mm diameter) holes into the burner tube that carries the gas flow. The holes are arranged in four rows, each having eight holes that are equally spaced around the tube circumference. Total entry area is ~25 mm^2 for the liquid and ~57 mm^2 for the gas. The length of the tube available for the combined two-phase gas-oil flow

(116 cm or 45.7 inches), which is equivalent to ~136x the tube inner diameter, is considered sufficient for the gas and oil to mix and develop into an annular two-phase flow.

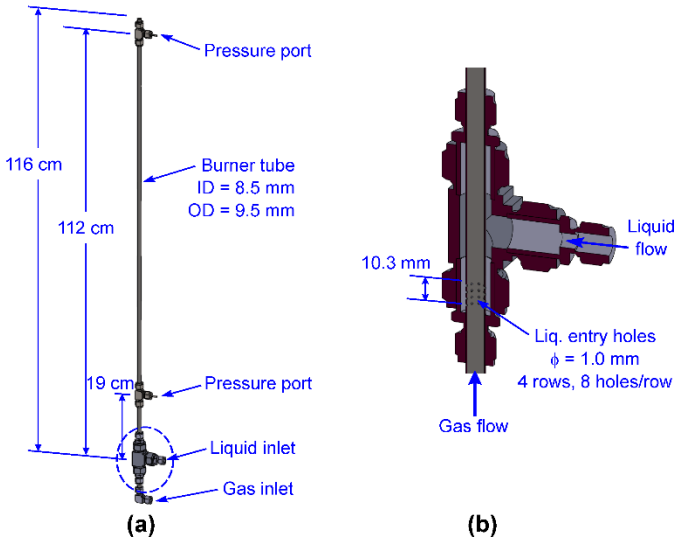

Figure 1. Schematic of (a) overall burner and (b) gas-liquid mixing tee.

For these experiments, gas reservoirs consist of the following: a six-pack of compressed methane (CH_4) cylinders connected to a single regulated manifold; a four-pack of compressed ethane (C_2H_6) cylinders connected to a single regulated manifold; and a 120-gallon propane tank with a regulator. Each of the regulated gas lines is equipped with a manual ball valve, a check valve, and a computer-interfaced mass flow controller (MFC). The MFC units (Alicat Scientific) have different flow ranges for each of the gases: 0 – 3000 SLPM for methane; 0 – 250 SLPM for ethane; and 0 – 1000 SLPM for propane. The three gases are mixed together downstream of the MFCs and sent to the burner. While most of the propane flow goes to the burner, a portion is split off before the MFC and regulated to provide fuel for a small pilot flame. Crude oil is pumped out of a 5-gallon bucket by a spur gear pump (Viking Pump, model SG-40514) with flow rate and pressure capacities of 21.2 LPM and 500 psi, respectively. A custom LabVIEW program and National Instruments CompactDAQ hardware are used for experimental control and data acquisition (DAQ). The LabVIEW program is used for two-way communication with the MFC

units to set desired flow and read actual flow. Desired liquid flow rate (expressed as a voltage) is communicated to a variable-speed drive system, which in turn controls the pump motor. A positive-displacement flow meter (FLOMEC, model OM015) measures and reports liquid flow rate to the DAQ computer.

Experiments were conducted at a NRL large-scale fire testing facility. The burner is set up in a test chamber known as an "IMO box". Though a standard IMO (International Maritime Organization) box has dimensions of 10 m × 10 m × 5 m, ours is actually 9.1 m × 9.1 m × 4.3 m (30 ft × 30 ft × 14 ft). The chamber has three doors, one on the east side near the northeast corner, which remained closed during all testing, and two on the south side, which remained open during testing for personnel to enter and exit and to safely observe the flame from outside. The roof of the chamber has a large opening (3 m × 3 m), which allowed the flame to establish its own natural height without interference from the roof.

Burn efficiency is quantified by collecting and measuring oil fallout on the ground surrounding the burner. It is not practical to collect and weigh all of the oil fallout over such a large area, thus we devised a setup to measure oil in strategic locations as shown in Figure 2. The burner is mounted vertically on a strut frame and support system, with the four base channels aligned in the NW, NE, SW, and SE directions. Aluminum weighing dishes (75-mm diameter) served as oil collection cups, which were positioned on thin steel bars using removable putty. Four of these steel bars, each with ten collection cups, were set up in the cardinal directions (N, E, S, and W) such that the cup nearest the burner on each of the bars was as close to the burner as possible. The radial distances of the cups are shown in Table 1. The positions were chosen to provide maximum resolution near the burner, where oil fallout is greatest, and less resolution farther away, where oil fallout rapidly decreases.

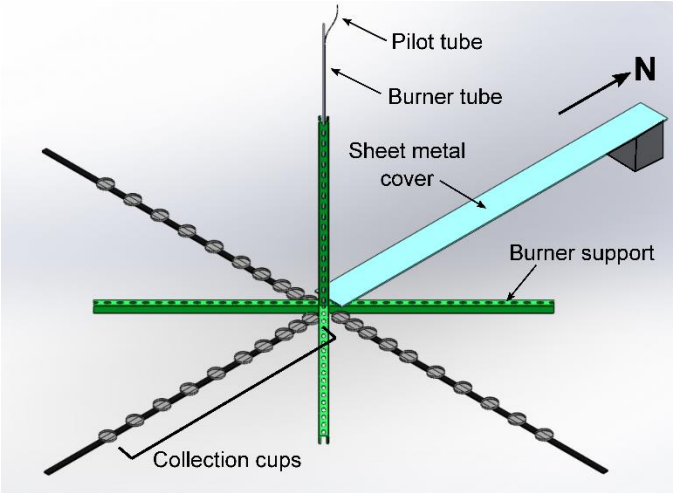

Figure 2. Isometric view of experimental setup for collection of oil fallout.

Table 1. Radial distances of cups for collection of oil fallout.

Cup #	Distance from burner center to cup center [cm]
1	8.9
2	16.5
3	24.1
4	35.6
5	47.0
6	62.2
7	77.5
8	92.7
9	108.0
10	123.2

Each experimental run lasted 4-5 minutes and required three people – one person to operate a digital video camera (mounted on a tripod just inside the SE chamber door) and observe the flame, one person to operate the DAQ computer, and one person to manage oil fallout collection. Before each test, oil collection cups were positioned and then covered with aluminum sheets, as shown in Figure 2 for one of the sets, to prevent oil from being collected during the transient startup of the flame. Once the propane pilot flame was ignited and the video recording was started, the DAQ computer was used to enable the gas mixture at low flow rate (typically 0.5 g/s) and then to gradually increase flow rate to the desired condition. The propane pilot, which ensured ignition of

the gas jet, was either shut off at this point or left on depending on the desired test conditions. Using the DAQ computer to turn on the liquid pump, oil flow was then initiated at the desired setpoint. After a short delay, oil reached the burner and began spraying out of the tube, at which point the already burning gas flame ensured ignition of the spray flame. Once the oil flow and spray flame were stabilized and at a nominally steady condition (typically after 1-2 minutes), the cover sheets over the collection cups were sequentially removed, as quickly as possible while remaining safe, to enable collection of oil fallout. At the instant each sheet was removed, a LabVIEW button was clicked to indicate in the data file that collection was initiated for the appropriate set of cups. Oil fallout was collected for 1-2 minutes (depending on flame condition and fallout rate), after which each metal cover sheet was replaced in the same sequence as they were removed to prevent oil collection during the transient shutdown of the flame. At the instant each sheet was replaced, a LabVIEW button was clicked to indicate in the data file that collection was terminated for the appropriate set of cups. Once all cups were covered again, the oil pump was stopped, then gas flow was gradually reduced to low flow rate and turned off. As quickly as possible, while being careful not to spill any of the collected oil, the cups were removed from the steel bars, placed in portable containers, and brought to a nearby building for immediate measurement of collected oil mass in each cup.

The fuels and flow conditions used for all tests are shown in Table 2. A mixture of methane, ethane, and propane, with mass fractions of 80 %, 5 %, and 15 %, respectively, was used to simulate well gases. Endicott crude oil, a light crude from the Beaufort Sea in the Alaska North Slope region, was used for all experiments. The approximate gas-oil ratio (GOR), in oil industry standard units, was above 1200 scf/bbl for both flow conditions. This value is much higher than the 500-scf/bbl threshold that Siddhamshetty et al. suggested is required for annular flow

(Siddhamshetty *et al.* 2019). Mass flow rates (MFRs) and associated standard deviations reported in Table 2**Error! Reference source not found.** were calculated from recorded data for relevant fallout collection period of each run.

Table 2. Test fuels and flow conditions

# Tests	13
Gas mixture	Methane/Ethane/Propane 80/5/15 % by mass
Gas MFR	3.0 ± 0.0 g/s
Crude oil	Endicott
Crude oil density*	873 kg/m^3 (API 30.6 degrees)
Crude oil viscosity*	17.5 cP
Crude oil MFR	(16.0 ± 0.5) g/s
Oil:Gas mass ratio	(5.3 ± 0.2) g/s
GOR	1216 scf/bbl

* Measured at NRL

In early testing, we found that the flame for the condition used in this study did not require any kind of pilot flame to remain ignited and stabilized, but for higher flow rates it was sometimes necessary. Thus, although it was not necessary, the pilot was used for seven of the thirteen tests in this study to evaluate whether it has any effect on the measured burn efficiency. The pilot flame is a small propane diffusion flame stabilized on a stainless steel tube with diameter of 1.5 mm (1/16 inch), positioned in the NE direction at a radial distance of approximately 7.5 cm (3 inches) and a height of approximately 12.5 cm (5 inches) from the top of the burner tube. This position was found, through trial and error, to be effective at stabilizing the spray flame and also kept the pilot flame itself from being entrained by the spray flame and extinguished.

DATA PROCESSING METHODS

Each experiment resulted in four profiles of collected oil mass, each with ten discrete points corresponding to the cup center locations, which were converted to profiles of differential oil mass

flux rate (in units of $g \cdot cm^{-2} \cdot s^{-1}$) by dividing each mass by the collection cup area (44.2 cm^2) and the relevant collection time for each respective direction. For each profile, a 100-point spline interpolation was performed to develop a smooth curve with increased spatial resolution. For one test run, the interpolated oil mass flux rate profiles for the four collection directions are shown in Figure 3 (left column).

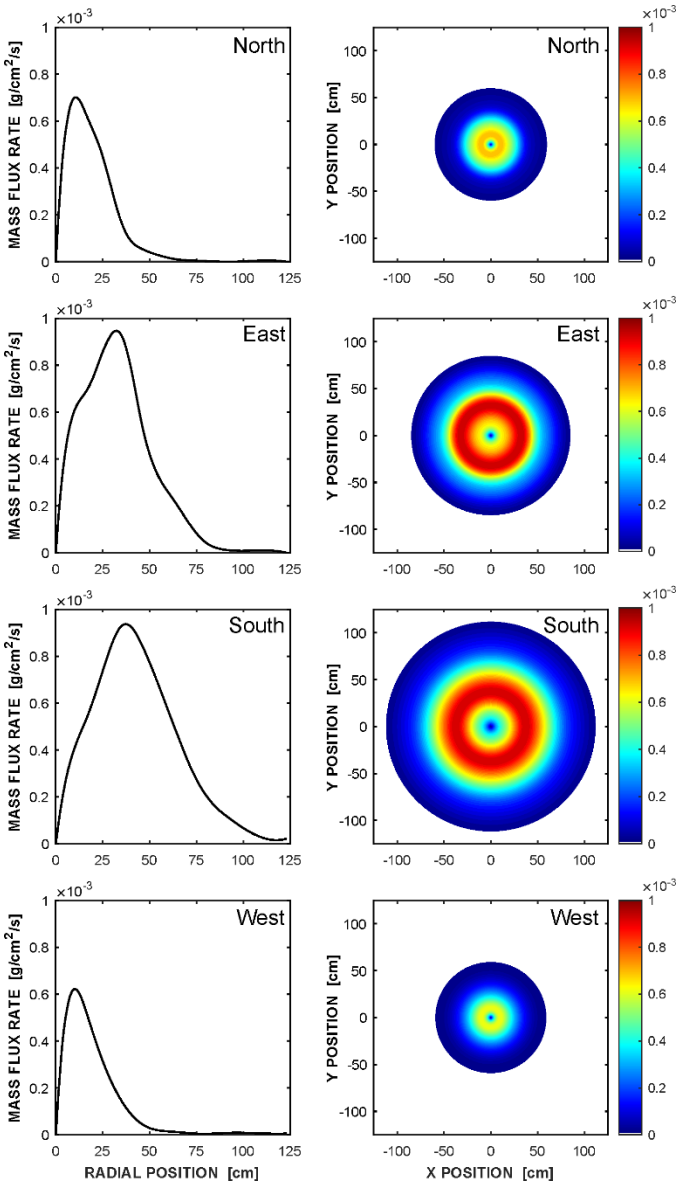

Figure 3. Oil mass flux rate profiles (left column) and full 2D distributions (right column) for the four collection directions from one burn efficiency test.

All four profiles have a similar overall shape, with an initial rapid increase in fallout with increasing radial distance, then a clear peak followed by a rapid decrease. The specific shapes and peak values of the profiles, however, are noticeably different, indicating a non-uniform distribution of oil fallout around the burner. The contour maps in Figure 3 (right column) illustrate what a full 2D distribution of mass flux rate would look like if each profile was assumed to be axisymmetric. For this particular test, oil fallout clearly favored the south direction, and to a lesser extent the east direction.

From the four individual flux profiles, an average profile is calculated and then numerically integrated (using trapezoid rule) over the 2D area around the burner to calculate a total fallout mass flow rate. Treating the average profile as axisymmetric, the integral simplifies to the expression in Equation 1, where $\dot{m}_f''$ is the fallout mass flux rate, $\dot{m}_f$ is the fallout mass flow rate, r is radial distance, and R is the maximum radial distance considered in the collection profiles.

$$\dot{m}_f = 2\pi \int_0^R \dot{m}_f'' \, r \, dr \qquad (1)$$

Fallout fraction (FF) and apparent burn efficiency (ABE) were then determined quite simply from Equations 2 and 3, respectively, where $\dot{m}_b$ is the average mass flow rate of oil through the burner over the entire oil collection time period.

$$FF = {\dot{m}_f}/{\dot{m}_b} \qquad (2)$$

$$ABE = \frac{\dot{m}_b - \dot{m}_f}{\dot{m}_b} = 1 - ({\dot{m}_f}/{\dot{m}_b}) \qquad (3)$$

RESULTS AND DISCUSSION

For this study, a total of thirteen gas/oil burn tests were conducted at a single flow condition (3 g/s gas, 16 g/s oil). Six of these were conducted with no pilot flame; the remaining seven tests were conducted using a small propane pilot as described above. Figure 4, which is an image recorded from one of the piloted runs on 14 May 2019, shows a tall, highly turbulent, highly

luminous spray flame. Clearly visible are the small pilot flame at the bottom right of the spray flame and an envelope of smoke around the spray flame. Just barely visible, below the lifted flame, is the pre-ignition gas/oil spray. It is difficult to see because of the short exposure time of the camera, which was chosen to prevent heavy saturation from the highly luminous flame. There do not appear to be any unburned oil droplets falling to the ground, but this is an artifact of the short exposure time setting. During the test, we could see unburned oil splattering out of the burner in the immediate vicinity, and oil fallout was clearly visible in the collection cups.

Figure 4. Gas/oil spray flame image, viewed from SE corner of test chamber.

The primary objective of this work was to develop and validate a method for measuring burn efficiency. The thirteen burn tests spanned a total time period of nearly three months, a temperature range of 32 °F, a wind speed range of nearly 20 mph, and a wide range of wind directions. Figure 5 shows the results for these experiments, both in terms of apparent burn efficiency and fallout fraction. First and foremost, we see that, on average, ABE for this condition was less than 70 % (FF was over 30 %). This is a significant finding, considering the potential implications for real-world wellhead burning scenarios. We believe that the reduced burn efficiency is due to a lower fraction of entrained liquid within the tube, meaning less liquid in the form of tiny droplets dispersed in the core gas flow and more liquid remaining in the annular film. The annular film atomizes upon exit from the burner tube and forms much larger droplets than those that are entrained inside the tube, thus presumably leading to lower burn efficiency. At this time, however, we cannot quantify these effects and are restricted to educated speculation.

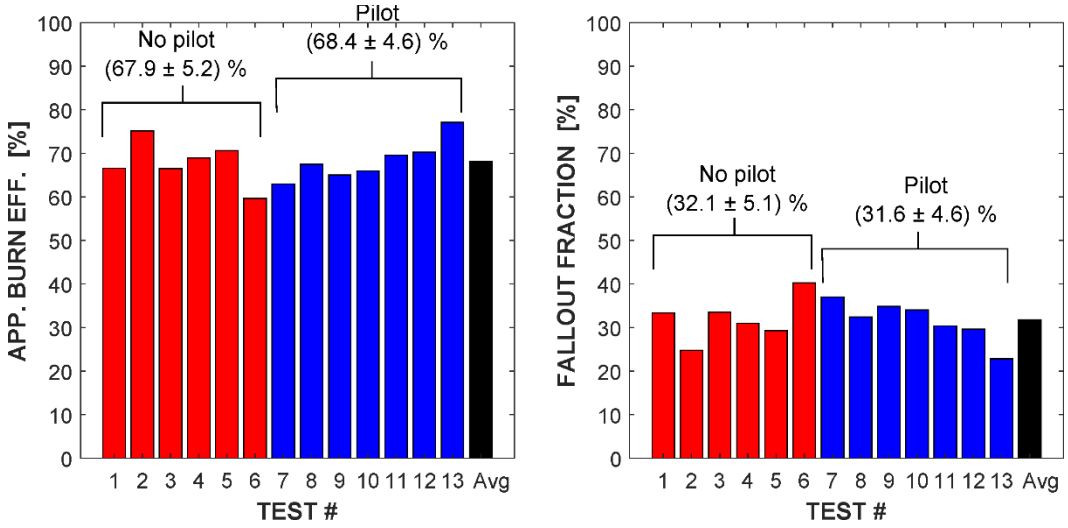

Figure 5. Apparent burn efficiency (left) and fallout fraction (right) for gas/oil spray flame tests, including both without and with a small propane pilot flame. Average values and standard deviations for each grouping are included.

As shown in Figure 5, there was little difference in the results whether or not a pilot flame was used. Average ABE was 67.9 % for the “no pilot” cases, 68.4 % for the “pilot” cases, and 68.2 %

overall (with standard deviation of 4.7 %) for the entire test set. Considering the scatter in the data, the difference between the cases is not at all statistically significant. Thus, we conclude that the pilot flame has no effect on the burn efficiency and only serves to stabilize the main spray flame.

The data were examined more closely for any correlations to weather conditions. There was no discernible correlation of burn efficiency to wind speed or direction, but there was a moderate correlation to temperature as shown in Figure 6. This is not surprising, since higher temperature is likely to cause faster evaporation of the crude oil as it is sprayed out of the burner and as it sits in the collection cups before the mass measurements. It is also possible that the higher oil viscosity associated with higher temperatures led to better atomization, but it is unknown if this effect would be significant enough to account for the observed changes in ABE.

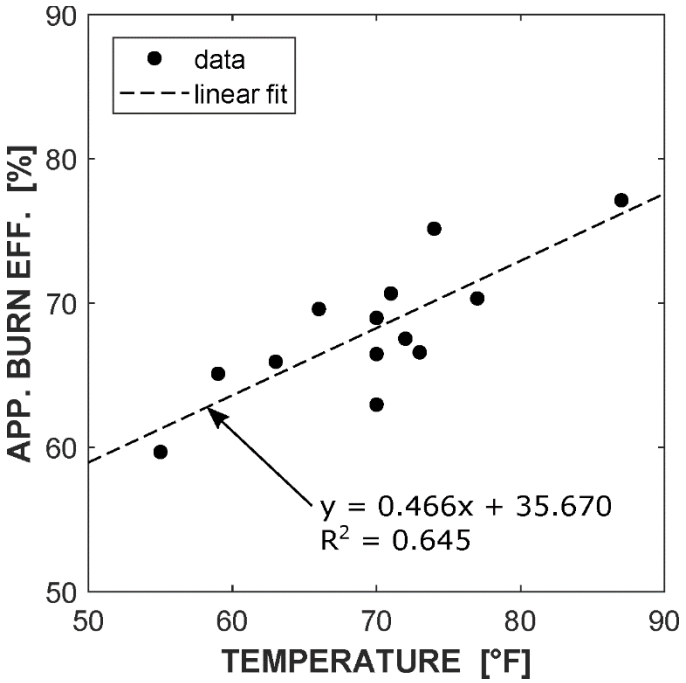

Figure 6. Apparent burn efficiency vs. temperature, including “no pilot” and “pilot” cases.

SUMMARY AND CONCLUSIONS

Voluntary ignition and burning gas/oil outflow is a potential response strategy for wellhead blowout events, but to be effective it requires high burn efficiency. There have been no studies,

however, in which burn efficiency has been directly quantified for a wellhead fire or anything that closely simulates one. Recognizing the importance of burn efficiency and the need to understand what affects it, we have developed a test setup and method at NRL to measure burn efficiency for spray flames that simulate scaled-down wellhead fires. The burner is designed to create two-phase annular and/or dispersed mist flow that simulates internal flow in an actual petroleum well. Gas and liquid flow are independently controlled so that it is possible to investigate a wide variety of two-phase flow conditions. For measurement of burn efficiency, we use aluminum weighing dishes to collect fallout of unburned oil and heavy combustion residuals around the burner. Furthermore, we devised a method of post-processing the collected mass data such that fallout only needs to be collected along four radial lines, from the burner out to a distance of ~125 cm, to enable estimation of the entire fallout field surrounding the burner. Total estimated fallout is compared with total liquid mass delivered through the burner to determine apparent burn efficiency (ABE). The measurement and data processing methods were used for a campaign of tests to examine the repeatability of the methods and sensitivity to weather conditions. In addition, we examined the effect of using a small pilot flame to stabilize the spray flame. For all tests, we used a mixture of methane, ethane, and propane with mass fractions of 80 %, 5 %, and 15 %, respectively as a representative gas mixture and Endicott (API = 30.6 degrees) as a representative crude oil. Below is a summary of the major findings of this work:

- Gas/oil spray flames were lifted (tens of cm), highly turbulent, and highly luminous. The flame height was approximately at the roofline of the test chamber (~7.5 m).
- There was a considerable amount of smoke surrounding the flame and there were clear vapor trails from partially burned droplets falling to the ground near the burner.

- Measured ABE and FF values were very similar both without and with a small propane pilot flame. On average over a total of thirteen tests, ABE was (68.2 ± 4.7) % and FF was (31.8 ± 4.7) %.
- There was a direct, seemingly linear correlation of ABE to air temperature.

The most important observation in this study was a measured burn efficiency significantly lower than 100 %, which would present a major issue for intentional wellhead ignition and burning. We believe this to be directly related to entrainment behavior in the two-phase flow within the burner tube. Though the data we currently have do not enable us to quantify entrainment, we conclude that the flow conditions used in this study led to an entrained liquid fraction that was significantly less than 100 %, meaning fewer tiny droplets dispersed in the core gas flow and more liquid in the annular film. With more liquid in the annular film, there is a larger fraction of large droplets formed when the two-phase flow exits the burner and likely a larger size distribution of those larger droplets, which leads to increased fallout and therefore reduced burn efficiency.

The next step in this work is to conduct parametric studies to quantify the effect of gas/oil flow conditions on fallout and burn efficiency, as well as to examine the effect of the oil properties by testing different crude oils. In parallel, we are also studying a laboratory-scale spray flame using a similar but scaled-down burner design to examine fundamental spray and combustion behavior. The overall objective is to develop a scalable computational model of these spray flames, validated using detailed laboratory-scale data, that can be used to predict burn efficiency for full-scale wellhead fires.

ACKNOWLEDGEMENTS

This study was funded in part by the U. S. Department of the Interior, Bureau of Safety and Environmental Enforcement (BSEE), through Inter-agency Agreement No. E15PG00022 with the Naval Research Laboratory (NRL), as part of the BSEE Oil Spill Response Research Program.

REFERENCES

Al-Sarkhi, A., Sarica, C., and Qureshi, B. 2012. Modeling of droplet entrainment in co-current annular two-phase flow: A new approach. International Journal of Multiphase Flow 39: pp. 21-28.

Aliyu, A. M., Almabrok, A. A., Baba, Y. D., Archibong, A. E., Lao, L. Y., Yeung, H., and Kim, K. C. 2017. Prediction of entrained droplet fraction in co-current annular gas-liquid flow in vertical pipes. Experimental Thermal and Fluid Science 85: pp. 287-304.

Azzopardi, B. J. 1997. Drops in annular two-phase flow. International Journal of Multiphase Flow 23: pp. 1-53.

Berna, C., Escriva, A., Munoz-Cobo, J. L., and Herranz, L. E. 2014. Review of droplet entrainment in annular flow: Interfacial waves and onset of entrainment. Progress in Nuclear Energy 74: pp. 14-43.

Berna, C., Escriva, A., Munoz-Cobo, J. L., and Herranz, L. E. 2015. Review of droplet entrainment in annular flow: Characterization of the entrained droplets. Progress in Nuclear Energy 79: pp. 64-86.

Hasan, R., and Kabir, S. 2018. Fluid Flow and Heat Transfer in Wellbores, Second Edition ed., Society of Petroleum Engineers, Richardson, TX, 2018.

Henstock, W. H., and Hanratty, T. J. 1976. Interfacial drag and height of wall layer in annular flows. AIChE Journal 22:6: pp. 990-1000.

Kataoka, I., Ishii, M., and Mishima, K. 1983. Generation and size distribution of droplet in annular two-phase flow. Journal of Fluids Engineering-Transactions of the ASME 105:2: pp. 230-238.

Kataoka, I., Ishii, M., and Nakayama, A. 2000. Entrainment and desposition rates of droplets in annular two-phase flow. International Journal of Heat and Mass Transfer 43:9: pp. 1573-1589.

Liu, L., and Bai, B. F. 2017. Generalization of droplet entrainment rate correlation for annular flow considering disturbance wave properties. Chemical Engineering Science 164: pp. 279-291.

Siddhamshetty, P., Ahammad, M., Hasan, R., and Kwon, J. 2019. Understanding wellhead ignition as a blowout response. Fuel 243: pp. 622-629.

Simmons, M. J. H., and Hanratty, T. J. 2001. Droplet size measurements in horizontal annular gas-liquid flow. International Journal of Multiphase Flow 27:5: pp. 861-883.

Steimes, J., and Hendrick, P. 2017. Measurement and prediction of droplet size in annular gas-liquid flows in aero-engine oil systems. International Journal of Multiphase Flow 93: pp. 84-91.

Taitel, Y., Bornea, D., and Dukler, A. E. 1980. Modeling flow pattern transitions for steady upward gas-liquid flow in vertical tubes. AIChE Journal 26:3: pp. 345-354.

Tatterson, D. F., Dallman, J. C., and Hanratty, T. J. 1977. Drop sizes in annular gas-liquid flows. AIChE Journal 23:1: pp. 68-76.

Wang, C., Zhao, N., Feng, Y., Sun, H. J., and Fang, L. D. 2018. Interfacial wave velocity of vertical gas-liquid annular flow at different system pressures. Experimental Thermal and Fluid Science 92: pp. 20-32.

Xue, T., Yang, L. X., Ge, P. H., and Qu, L. Q. 2015. Error analysis and liquid film thickness measurement in gas-liquid annular flow. Optik 126:20: pp. 2674-2678.

Zhang, H. B., and Hewitt, G. F. 2017. New models of droplet deposition and entrainment for prediction of liquid film flow in vertical annuli. Applied Thermal Engineering 113: pp. 362-372.